Turkish Journal of Electrical Engineering & Computer Sciences

http://journals.tubitak.gov.tr/elektrik/

Research Article

Turk J Elec Eng & Comp Sci
(2016) 24: 580 – 589

doi:10.3906/elk-1310-245

Sensorless velocity and direction angle control of an unmanned vehicle

Abdullah BAŞÇİ, Adnan DERDİYOK*
Department of Electrical and Electronics Engineering, Atatürk University, Erzurum, Turkey

Received: 30.10.2013 • **Accepted/Published Online:** 18.12.2013 • **Final Version:** 05.02.2016

Abstract: In this paper an observer based on measured and estimated currents and a kinematic model is designed to estimate the velocity and direction angle of an unmanned vehicle (UV). The Lyapunov stability theory is used to establish the stability conditions for the observer. It is shown that the observer will converge in a finite time and the observer gains satisfy the constraints of the stability conditions. The observed velocity and direction angle are used in the closed loop instead of measured ones for sensorless control of the UV. The velocity and direction angle control of the UV are carried out by a well-tuned PI controller. The experimental results show that the proposed observer can be perfectly implemented for sensorless control without using a mechanical sensor, and satisfying results are obtained. In the experiment, command voltages are used rather than measured ones, and therefore only current sensors are needed for the proposed algorithm.

Key words: Sensorless control, vehicle system, direction control, path tracking

1. Introduction

Unmanned vehicles (UVs) have recently been used in various applications such as transportation, planetary exploration, mining, military operation, etc. The movements of UVs are performed using electrical motors. Electrical motors consume a large percentage of the provided electrical energy in the UV's system. Therefore, the motion control of the electrical motors plays an important role in electrical energy consumption. The motion control of the electrical motors requires not only an accurate knowledge of the rotor position, but also information about the rotor speed for closed-loop control. Thus, position sensors such as an optical encoder and a tachogenerator need to be mounted onto the motor shaft [1,2]. However, the installation of these position sensors has some drawbacks related to increasing cost, size, weight, and wiring complexity of the motor drive systems. From the viewpoint of system reliability, mounting position sensors on the rotors will reduce the mechanical robustness of electric machines, particularly in hard work environments [3,4]. To overcome these drawbacks, significant research in the last decades [5,6] has gone into the development of sensorless drives that have a comparable or similar dynamic performance to sensor-based drives. The advantages of sensorless control are not only the reductions in cost and size, but also in the simplification of the procedures of system assembly and maintenance as well as improved reliability by eliminating the position sensor and related cabling connections [7–10].

In the literature, many research efforts have been made for estimating the speed of electric motors in sensorless speed control. The model reference adaptive system methods [11,12] are based on the comparison between the outputs of 2 estimates. The output errors are then used to drive a suitable adaptation mechanism

*Correspondence: derdiyok@atauni.edu.tr

that generates the estimated speed. These schemes require integration and the system performance is limited by parameter variations. The Kalman filter approaches [13–16] are known to be able to get accurate speed information, but they have some inherent disadvantages, such as the influence of noise and a large computational burden. Sliding mode observers [17–20], due to their order reduction, robustness to disturbances, good dynamic performance, simple algorithms, and low sensitivity to parameter variations, are widely used in sensorless control applications. Speed estimation algorithms based on neural networks have shown that they can achieve high performance, but they are relatively complicated and require a long computational time [21–23].

In this paper, an observer based on measured and estimated currents and a kinematic model is designed to estimate the velocity and direction angle of an UV. The observed velocity and direction angle are used in the closed loop instead of the measured ones for sensorless control of an UV. The experimental results obtained prove that the observer is robust to complex references and can also follow command trajectories very well.

2. Design of the UV

The deferentially driven UV considered in this paper is depicted in Figure 1. It consists of a mobile platform with 2 differential driving wheels mounted on the same axis, and a free wheel to keep the platform stable.

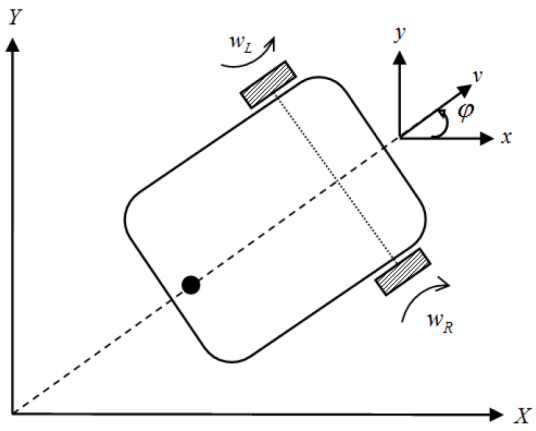

Figure 1. Vehicle model and its coordinate system.

We can write the following kinematic equations from the motion equations of the vehicle [24,25]:

$$v_R = R \cdot \omega_R, \tag{1}$$

$$v_L = R \cdot \omega_L, \tag{2}$$

$$v = \frac{v_R + v_L}{2} = \frac{R}{2} \quad (\omega_R + \omega_L), \tag{3}$$

$$\frac{d\phi}{dt} = \frac{R}{L} \quad (\omega_R - \omega_L), \tag{4}$$

$$\frac{dx}{dt} = v_x = v \cdot \cos \ (\ \phi) = \frac{R}{2} \ (\ \omega_R + \omega_L) \cos \ (\phi) \ , \tag{5}$$

$$\frac{dy}{dt} = v_y = v \cdot \sin\ (\ \phi) = \frac{R}{2}\ (\ \omega_R + \omega_L) \sin\ (\phi)\ , \tag{6}$$

where L is the distance between the wheels and R is the radius of the wheel. v_R and v_L represent the linear velocity of the right and left wheels, w_R and w_L are the right and left wheels' angular velocity, and v and ϕ are the vehicle linear velocity and the vehicle direction angle, respectively. v_x is the velocity component in x direction and v_y is the velocity component in y direction.

The motion and the orientation of the vehicle are achieved by independent actuators of the left and right wheels, and each wheel is independent and driven by a servo motor through a gearbox as shown in Figure 2.

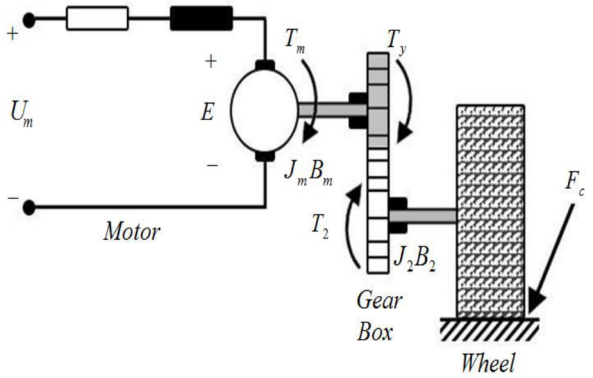

Figure 2. Drive system for each wheel of the vehicle.

The torque transferred from the motor to the gearbox can be written as follows:

$$T_m = J_m \frac{d^2\theta_m}{dt^2} + B_m \frac{d\theta_m}{dt} + T_{Load}, \tag{7}$$

$$T_{Load} = n^2 J_2 \frac{d^2\theta_m}{dt^2} + n^2 B_2 \frac{d\theta_m}{dt} + nF_c \frac{\dot{\theta}}{\left|\dot{\theta}\right|}, \tag{8}$$

where J_m is the inertia moment, B_m is the friction coefficient, θ_m is the angle of rotation, n is the reduction ratio of the gearbox, and F_c is the coulomb torque constant. From Eqs. (7) and (8):

$$T_m = (J_m + n^2 J_2)\frac{d^2\theta_m}{dt^2} + (B_m + n^2 B_2)\frac{d\theta}{dt} + nF_c sign(\dot{\theta}_m), \tag{9}$$

$$\eta_1 = \frac{B_m + n^2 B_2}{J_m + n^2 J_2}, \quad \eta_2 = \frac{nF_c}{J_m + n^2 J_2}, \quad \eta_3 = \frac{1}{J_m + n^2 J_2}, \tag{10}$$

$$\frac{d^2\theta_m}{dt^2} = -\eta_1 \frac{d\theta_m}{dt} - \eta_2 sign(\dot{\theta}_m) + \eta_3 T_m). \tag{11}$$

To represent the vehicle equation in the state space, we select the state vector as:

$$x_1 = v, \quad x_2 = \dot{\theta}, \quad x_3 = \theta, \tag{12}$$

and then the above equations, which describe the dynamics of the vehicle, can be written in a more convenient matrix form as:

$$\begin{bmatrix} \dot{x}_1 \\ \dot{x}_2 \\ \dot{x}_3 \end{bmatrix} = \begin{bmatrix} -\eta_1 x_1 - \eta_2 \frac{R}{2}(sign(g_1(x)) + sign(g_2(x))) \\ -\eta_1 x_2 - \eta_2 \frac{R}{2}(sign(g_1(x)) + sign(g_2(x))) \\ x_2 \end{bmatrix} + R\eta_3 \begin{bmatrix} 1/2 & 1/2 \\ 1/L & -1/L \\ 0 & 0 \end{bmatrix} \begin{bmatrix} T_R \\ T_L \end{bmatrix}, \tag{13}$$

where

$$g_1(x) = \frac{1}{R}x_1 + \frac{L}{2R}x_2, \quad g_2(x) = \frac{1}{R}x_1 - \frac{L}{2R}x_2. \tag{14}$$

Thus, our system can be shown in nonlinear matrix form as:

$$\frac{dx}{dt} = f(x) + B(u), \tag{15}$$

where $u = [T_R T_L]^T$, $f(x)$, and B are the matrices in Eq. (13).

3. Observer model

A closed-loop observer model is proposed to estimate the velocity and direction angle of the UV, and its equations are driven from the current errors of each motor and the kinematic model of vehicle. When the observer minimizes the error between the estimated and measured currents, the estimated states approach the real ones, and then the velocity and direction angle can be calculated correctly. The motor current equations and related observer equations for each wheel driving motor are given as follows:

$$\left.\begin{aligned} \tfrac{di_R}{dt} &= k_1 U_R - k_2 i_R - E_a \\ \tfrac{di_L}{dt} &= k_1 U_L - k_2 i_L - E_b \end{aligned}\right\} \tag{16}$$

$$\left.\begin{aligned} \tfrac{d\hat{i}_R}{dt} &= k_1 U_R - k_2 \hat{i}_R - \hat{U}_a \\ \tfrac{d\hat{i}_L}{dt} &= k_1 U_L - k_2 \hat{i}_L - \hat{U}_b \end{aligned}\right\} \tag{17}$$

where U_R and U_L are the input voltage for the left and right motors, i_R and i_L are the left and right motors' measured currents, $\hat{i}_R$ and $\hat{i}_L$ are the estimated currents, and $k_1 = 1/L$ and $k_2 = R/L$ are constants. $\hat{U}_a$ and $\hat{U}_b$ are the observer inputs and can be expressed as follows:

$$\hat{U}_a = K_a sign(s_R),$$

$$\hat{U}_b = K_b sign(s_L), \tag{18}$$

where s_R and s_L are defined as:

$$s_R = \hat{i}_R - i_R,$$

$$s_L = \hat{i}_L - i_L. \tag{19}$$

s_R and s_L are current estimation errors, and K_a and K_b are gains. To provide the Lyapunov stability criteria, the candidate Lyapunov function is selected as:

$$V = \frac{1}{2}\left(s_R^2 + s_L^2\right) \tag{20}$$

which is positive definite, but for stability its derivative needs to be negative definite. Taking the time derivative of the Lyapunov function gives:

$$\begin{aligned}\dot{V} &= s_R\dot{s}_R + s_L\dot{s}_L = s_R\left(\frac{U_R}{L} - \frac{R\hat{i}_R}{L} - \frac{K_a sign\left(s_R\right)}{L} - \frac{U_R}{L} + \frac{Ri_R}{L} + \frac{E_a}{L}\right)\\ &+s_L\left(\frac{U_L}{L} - \frac{R\hat{i}_L}{L} - \frac{K_b sign(s_L)}{L} - \frac{U_L}{L} + \frac{Ri_L}{L} + \frac{E_b}{L}\right)\end{aligned} \tag{21}$$

$$\dot{V} = -\frac{R}{L}s_{R}s_R - \frac{R}{L}s_{L}s_L - \frac{1}{L}K_a s_R sign(s_R) - \frac{1}{L}K_b s_L sign(s_L) + \frac{1}{L}E_a s_R + \frac{1}{L}E_b s_L \tag{22}$$

As seen from Eq. (22), the first two terms are negative definite, and if gains K_a and K_b are selected to be large enough, then stability condition $\dot{V} < 0$ can be satisfied and the error dynamic will converge in finite time. If the current estimation errors are $S_R \to 0$ and $S_L \to 0$, then the observer control inputs can be expressed as $\hat{U}_a \cong E_a$ and $\hat{U}_b \cong E_b$. The back EMF equations of each motor are:

$$E_a = \lambda w_R \text{ and } E_b = \lambda w_L. \tag{23}$$

The observer control inputs can then be written as follows:

$$\hat{U}_a = \lambda \hat{w}_R \text{ and } \hat{U}_b = \lambda \hat{w}_L. \tag{24}$$

From the kinematic equations of the UV, estimation equations for the velocity and direction angle are expressed as:

$$\hat{\nu} = \frac{\hat{\nu}_R + \hat{\nu}_L}{2} = \frac{R}{2}\left(\hat{w}_R + \hat{w}_L\right) \tag{25}$$

$$\dot{\hat{\varphi}} = \frac{R}{L}\left(\hat{w}_R - \hat{w}_L\right), \tag{26}$$

where the following equations can be written from Eq. (21):

$$\hat{w}_R + \hat{w}_L = \frac{1}{\lambda}\left(\hat{U}_a + \hat{U}_b\right) \tag{27}$$

$$\hat{w}_R - \hat{w}_L = \frac{1}{\lambda}\left(\hat{U}_a - \hat{U}_b\right) \tag{28}$$

Low-pass filters are used to get continuous rotational speeds ($\hat{w}_R\hat{w}_L$) from discontinuous $\hat{U}_a$ and $\hat{U}_b$ signals.The block diagram of the sensorless control of the UV is given in Figure 3. PI controllers, which have well-tuned parameters, are used to control the velocity and direction angle of the UV. The controllers produce u_v and u_ϕ by using comparator errors to calculate each motor reference torque command, which are then used to control each motor's angular velocity.

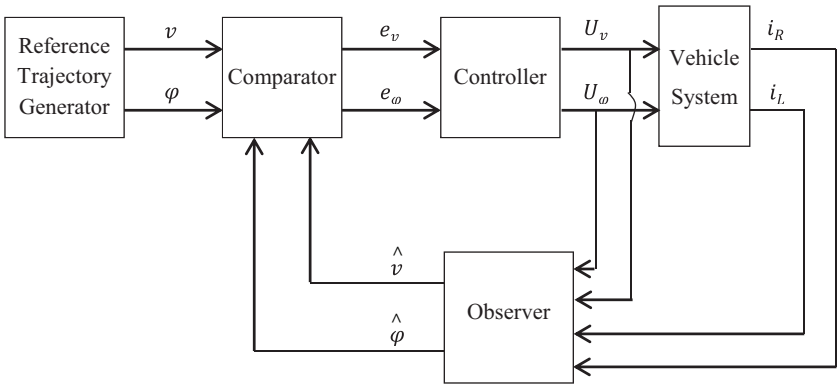

Figure 3. Block diagram of the vehicle control system.

4. Experimental results

In this section, the proposed observer is executed on an UV (shown in Figure 4) to apply the algorithm experimentally. Experimental results show the effectiveness of the proposed observer. The dimensions of the UV are 0.80 m $\times$ 0.45 m $\times$ 0.70 m, and its weight is 17 kg with load. The UV is equipped with 2 fast response servo motors with incremental encoders counting 500 pulses/turn, speed reduction gearboxes, an encoder interface card, a PC-DAQ, and analog motor driver circuits. The software is run on a 3.0 GHz Pentium VI, using the Windows real-time operation system.

Figure 4. Laboratory experimental vehicle.

The vehicle's real velocity and direction angle are obtained using motor rotor position sensors attached to each motor shaft, and the motor currents are measured with current sensors. The validation of the observer is achieved by comparing the estimated velocity, direction angle, and current of each motor against the real ones and the experimental results of the vehicle system are shown.

In the first experiment, the performance of the proposed observer is tested in the closed-loop control of the UV for square wave velocity and sinusoidal direction angle references. The square wave reference is important to test the performance of the observer for step changes. The references, measured and estimated values of the velocity and direction angle along with errors of velocity and direction angle, estimated and measured motor currents, motor commands, and trajectories are presented in Figure 5. It can be seen that the estimated currents have very good agreement with the measured currents and that the observer provides accurate tracking of the measured velocity, direction angle, and the calculated trajectory by using the estimated velocity and direction angle matching the reference trajectory with small error, which verified the effectiveness of the observer.

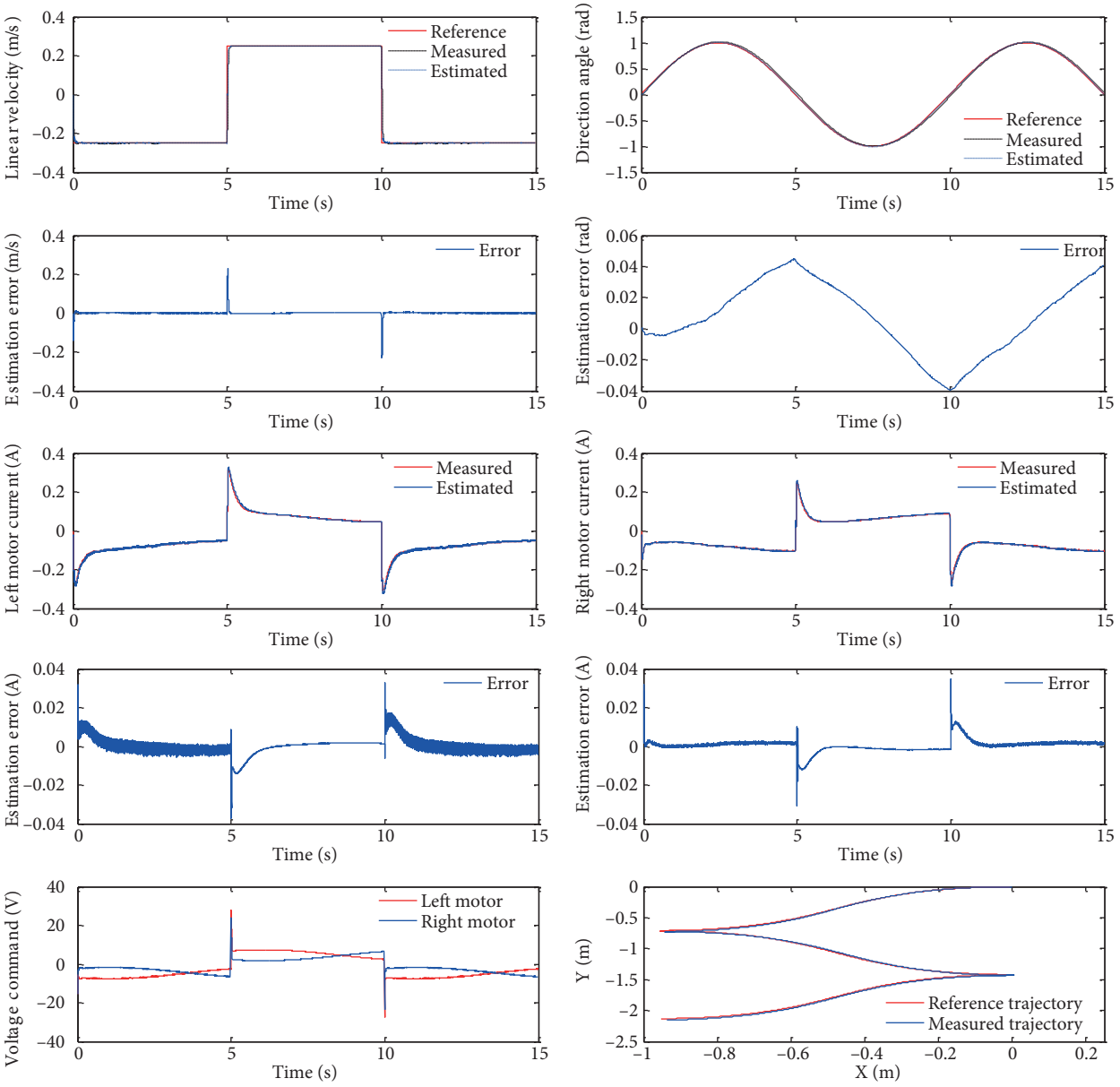

Figure 5. Experimental results for the square wave velocity and sinusoidal direction angle references.

In the second case, a sawtooth wave velocity and triangle direction angle references are chosen. The real and estimated velocity and direction angle along with the estimation errors are presented in Figure 6. As shown

in the figure, the estimated currents of each motor could keep up with the measured ones well and the vehicle follows the reference trajectory with small error.

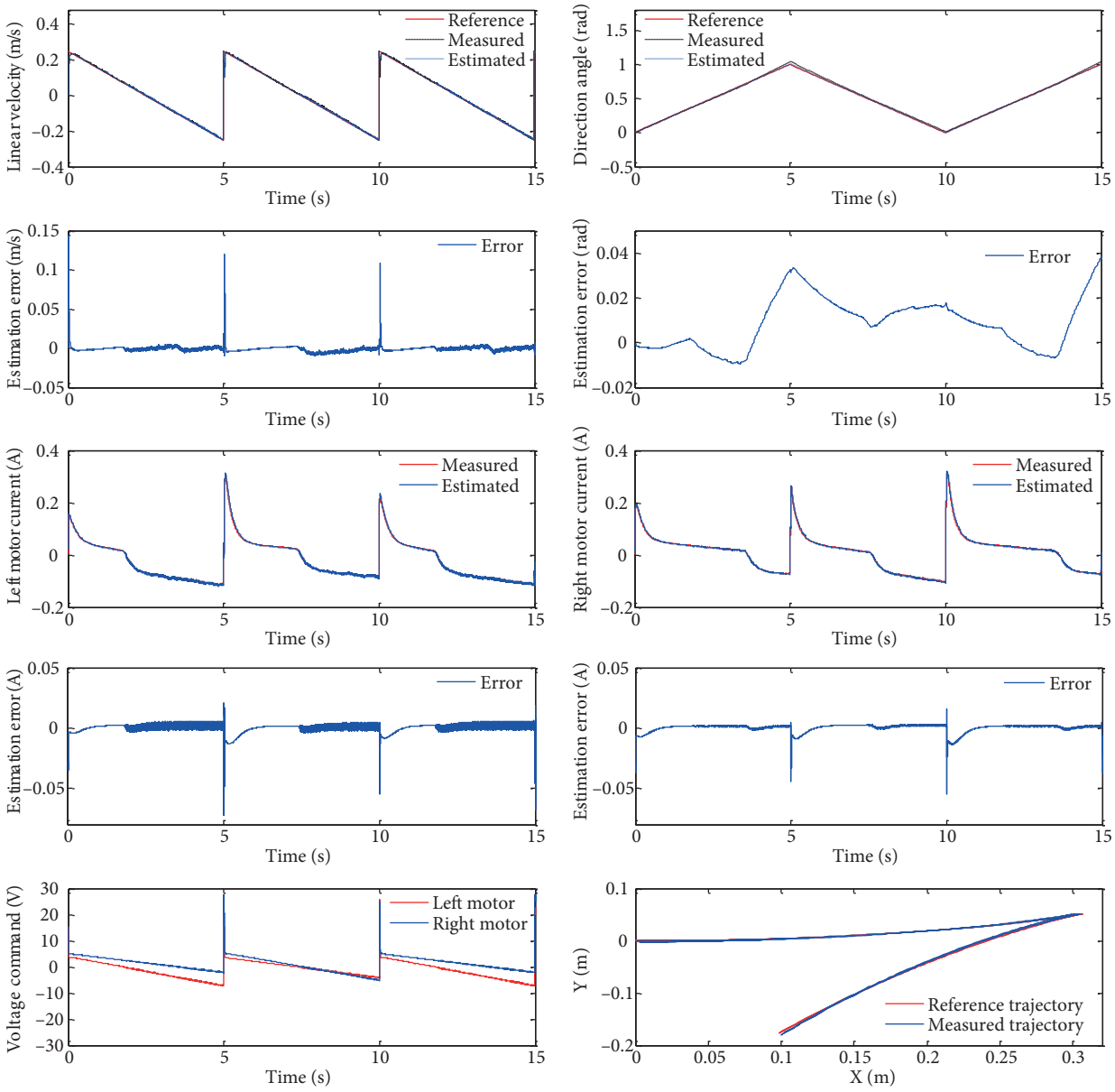

Figure 6. Experimental results for the sawtooth velocity and triangle direction angle references.

The estimation errors are defined as the errors between the estimated and actual values of the velocity and direction angle of the UV. As shown in Figures 5 and 6, if we disregard the errors occurring at step changes in the reference velocity, the maximum estimation percentage of errors of the square wave and sawtooth velocity is 2.31% and 1.13%, respectively. In a similar way, the maximum estimation percentage of errors of the sinusoidal and triangle direction angle is 4.23% and 3.86%, respectively.

5. Conclusion

A sensorless control algorithm is applied to the velocity and direction angle of an UV. Velocity and direction angle estimation are based on measured and estimated currents of the driving motor and a kinematic model of the vehicle. Complex references are chosen for the velocity and direction angle control of the UV to validate the performance of the proposed observer algorithm, and experimental results show that the vehicle's real velocity and direction angle are perfectly tracked and the estimation errors are very small.

References

[1] Liu H, Li S. Speed control for PMSM servo system using predictive functional control and extended state observer. IEEE T Ind Electron 2012; 59: 1171–1183.

[2] Sergeant P, De Belie F, Melkebeek J. Rotor geometry design of interior PMSMs with and without flux barriers for more accurate sensorless control. IEEE T Ind Electron 2012; 59: 2457–2465.

[3] Pacas M. Sensorless drives in industrial applications. IEEE Ind Electron Mag 2011; 5: 16–23.

[4] Raca D, Garcia P, Reigosa DD, Fernando B, Lorenz RD. Carrier-signal selection for sensorless control of PM synchronous machines at zero and very low speeds. IEEE T Ind Appl 2010; 46: 167–178.

[5] Orlowska-Kowalska T, Dybkowski M. Stator-current-based MRAS estimator for a wide range speed-sensorless induction-motor drive. IEEE T Ind Electron 2010; 57: 1296–1308.

[6] Tomei P, Verrelli CM. Observer-based speed tracking control for sensorless permanent magnet synchronous motors with unknown load torque. IEEE T Automat Contr 2011; 56: 1484–1488.

[7] Luenberger DG. An introduction to observers. IEEE T Automat Contr 1971; 16: 596–602.

[8] Lascu C, Boldea I, Blaabjerg F. Comparative study of adaptive and inherently sensorless observers for variable-speed induction motor drives. IEEE T Ind Electron 2006; 53: 57–65.

[9] Aksoy S, Mühürcü A. Induction motor, state estimation, extended Kalman filtering, recurrent neural networks. Turk J Electr Eng Co 2011; 19: 861–875.

[10] Davari SA, Khaburi DA, Wang F, Kennel R. Robust sensorless predictive control of induction motors with sliding mode voltage model observer. Turk J Electr Eng Co 2013; 21: 1539–1552.

[11] Kang J, Zeng X, Wu Y, Hu D. Study of position sensorless control of PMSM based on MRAS. In: Proceedings of the IEEE Industrial Technology Conference; 10–13 February 2009; Gippsland, Australia. New York, NY, USA: IEEE. pp. 1–4.

[12] Abu-Rub H, Khan MR, Iqbal A, Ahmed SM. MRAS-based sensorless control of a five-phase induction motor drive with a predictive adaptive model. In: Proceedings of the ISIE; 4–7 July 2010; Bari, Italy. New York, NY, USA: IEEE. pp. 3089–3094.

[13] Praesomboon S, Athaphaisal S, Yimman S, Boontawan R, Dejhan K. Sensorless speed control of DC servo motor using Kalman filter. In: Proceedings of the 7th International Conference on Information, Communications, and Signal Processing; 2009; Macau. New York, NY, USA: IEEE. pp. 1–5.

[14] Boizot N, Busvelle E, Gauthier JP, Sachau J. Adaptive gain extended Kalman filter: Application to a series-connected DC motor. In: Proceedings of the Conference on Systems and Control; 2007; Marrakech, Morocco. pp. 1–7.

[15] Janiszewski D. Load torque estimation in sensorless PMSM drive using unscented Kalmana filter. In: Proceedings of the ISIE; 27–30 June 2011; Gdansk, Poland. New York, NY, USA: IEEE. pp. 643–648.

[16] Jang JS, Park BG, Kim TS, Lee DM, Hyun DS. Parallel reduced-order extended Kalman filter for PMSM sensorless drives. In: Proceedings of the IEEE Industrial Electronics Society Annual Conference; 10–13 November 2008; Orlando, FL, USA. New York, NY, USA: IEEE. pp. 1326–1331.

[17] Lascu C, Boldea I, Blaabjerg F. A class of speed-sensorless sliding mode observers for high-performance induction motor drives. IEEE T Ind Electron 2009; 56: 3394–3403.

[18] Chu JB, Hu YW, Huang WX, Wang MJ, Yang JF, Shi YX. An improved sliding mode observer for position sensorless vector control drive of PMSM. In: Proceedings of the IEEE Power Electronics and Motion Control Conference; 17–20 May 2009; Wuhan, China. New York, NY, USA: IEEE. pp. 1898–1902.

[19] Chi S, Zhang Z, Xu LY. Sliding mode sensorless control of direct drive PM synchronous motors for washing machine applications. IEEE T Ind Appl 2009; 45: 582–590.

[20] Veluvolu KC, Soh YC. High-gain observers with sliding mode for state and unknown input estimations. IEEE T Ind Electron 2009; 56: 3386–3393.

[21] Karanayil B, Rahman MF, Grantham C. Online stator and rotor resistance estimation scheme artificial neural networks for vector controlled speed sensorless induction motor drive. IEEE T Ind Elect 2007; 54: 167–176.

[22] Guo HJ, Sagawa S, Watanabe T, Ichinokura O. Sensorless driving method of permanent-magnet synchronous motors based on neural networks. IEEE T Magn 2003; 39: 3247–3249.

[23] Partal S, Şenol İ, Bakan AF, Bekiroğlu KN. Online speed control of a brushless AC servomotor based on artificial neural networks. Turk J Electr Eng Co 2011; 19: 373–383.

[24] Ertuğrul M, Şabanoviç A, Kaynak O. Various VSS techniques on the control of automated guided vehicles. Gebze, Turkey: TÜBİTAK Marmara Research Center Technical Report, 1994.

[25] Başçi A, Derdiyok A. Real-time velocity and direction angle control of an automated guided vehicle. Int J Robot Autom 2014; 29: 227–233.